

Experimental Investigation of Some Consequences of Low Velocity Impacts in the Chaotic Dynamics of a Mechanical System

A. Stensson and A. B. Nordmark

Phil. Trans. R. Soc. Lond. A 1994 **347**, 439-448
doi: 10.1098/rsta.1994.0053

Email alerting service

Receive free email alerts when new articles cite this article - sign up in the box at the top right-hand corner of the article or click [here](#)

To subscribe to *Phil. Trans. R. Soc. Lond. A* go to:
<http://rsta.royalsocietypublishing.org/subscriptions>

Experimental investigation of some consequences of low velocity impacts in the chaotic dynamics of a mechanical system

BY A. STENSSON¹ AND A. B. NORDMARK²

¹*Department of Mechanical Engineering, Luleå University of Technology,
S-97187 Luleå, Sweden*

²*Department of Mechanics, Royal Institute of Technology,
S-10044 Stockholm, Sweden*

An experimental investigation of an impacting system is presented. The dynamical behaviour of the experimental system is compared with that of a simple model system using the common notion of an instantaneous velocity change, with outgoing velocity being a function of incoming velocity. This type of model has singularities in the Poincaré mappings used to describe the dynamics and this produces effects not found in smooth dynamical systems. The major contribution of this study is to show that these effects are also characteristic of the experimental system. One of those effects is that the chaotic attractors exhibit certain geometric features. The accuracy of the measurements made it possible to identify this effect in the experiment. As the experimental system is more complicated than the model, our measurements support that these features are present in more complex models. Thus it is demonstrated that the geometric features provide a diagnostic tool for impact studies.

1. Introduction

To prevent large amplitude oscillations in mechanical structures, limiters of displacement are often applied. A typical example is the bump-stop in a wheel suspension system of a vehicle. This implies that the mechanical parts will make contact with each other. It is important to find out how this contact can influence the behaviour of the system.

Models of impacting systems have been studied theoretically during the last ten years; some examples are Holmes (1982); Shaw & Holmes (1983*a-c*); Thompson & Ghaffari (1982, 1983); Thompson (1983); Lo (1985); Shaw (1985*a*); Isomäki *et al.* (1985); Whiston (1987*a, b*, 1992); Peterka (1992); Sung & Yu (1992); Nordmark (1991, 1992*a, b*). Studies have been made on elastic and inelastic impacts, on systems with low and large damping, harmonic and random excitation etc. and experimental investigations are shown in some cases (Wood & Byrne 1982; Moon & Shaw 1983; Shaw 1985*b*; Kowalik *et al.* 1988; Chen & Semercigil 1992; Bayly & Virgin 1993).

A model commonly used when studying the dynamics of impacting systems is one in which velocity changes instantly, with outgoing velocity being a function of incoming velocity. This type of model leads to singularities in the Poincaré mappings used to describe the dynamics. It has been found that low velocity impacts have a

Phil. Trans. R. Soc. Lond. A (1994) **347**, 439–448

© 1994 The Royal Society

Printed in Great Britain

439

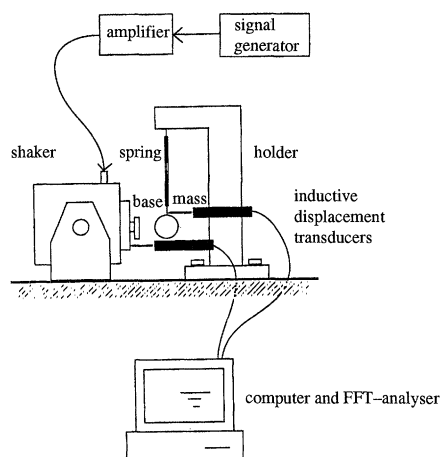


Figure 1. The experimental setup.

destabilizing effect on the dynamics (Nordmark 1991, 1992*a, b*). A strong indicator of this is that the chaotic attractors exhibit certain geometric features. These are generally found in numerical simulations (Nordmark 1992*a*). In this paper a simple experimental system is used to evaluate whether the special features observed in theoretical and numerical studies are present in the physical system. That would support the assumption that the model with sudden impact is correct.

The goal of this investigation is to measure the system behaviour with sufficient resolution for these geometric features to be decisively recognized.

The experimental system considered is shown in figure 1. It consists of one part that is moving sinusoidally and another part initially at rest. The part initially at rest is a mass attached to a spring. The spring is clamped in a holder. The system is excited by a moving part called the base. The motion of the base is harmonic and the amplitude and the frequency of the base can be varied. The equilibrium positions of the mass and the base are separated. Thus, for small amplitudes of the base the mass can remain at rest.

The experimental system is modelled as a simple spring–mass system impacting with a moving base. This model is investigated by using numerical simulations.

2. The mathematical model

A model with one degree of freedom is considered. The dynamics of the mass–beam system were assumed to be mainly dominated by the first mode, as the other modes will be damped out quickly and the excitation frequency is well below the higher natural frequencies. The beam is modelled as a linear spring for small deflections. The system is excited by a base that vibrates harmonically.

The system variables and parameters are shown in figure 2. They are non-dimensionalized as follows. The motion of the system is described by $x = (y - z)/b$. With this choice, impacts will always occur at $x = -1$. Time is scaled so the period of the base motion is 2π , i.e. $\tau = \omega t$. The amplitude of the base is scaled by the equilibrium stand-off distance, i.e. $a = A/b$. The properties of the spring are measured by the ratio of the driving frequency and the natural frequency, $w = \omega/\omega_n$, and a non-dimensional damping constant, D .

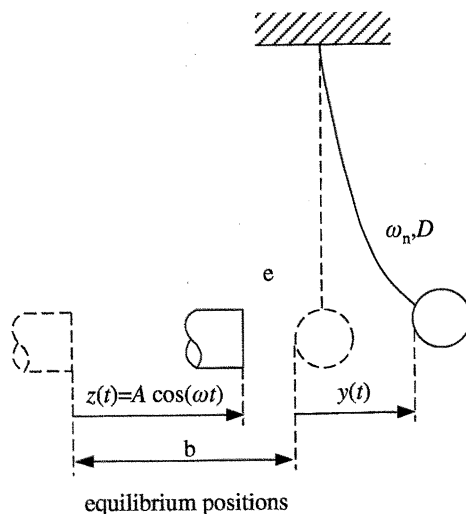


Figure 2. The significant parameters.

The impact is modelled to be instantaneous and controlled by a coefficient of restitution, e . Thus we arrive at the following equations:

$$\frac{d^2x}{d\tau^2} + \frac{2D}{w} \frac{dx}{d\tau} + \frac{1}{w^2} x = a \left\{ \left(1 - \frac{1}{w^2} \right) \cos \tau + \frac{2D}{w} \sin \tau \right\}, \quad (1)$$

$$x \geq -1, \quad (2)$$

and $(dx/d\tau)_{\text{just after impact (at } x=-1)} = -e(dx/d\tau)_{\text{just before impact (at } x=-1)}$. (3)

3. Effects of low velocity impact

The effect of low velocity impact on the dynamics can be demonstrated by considering the Poincaré mapping. Here, as in the following, a mapping of position and velocity at a chosen constant phase relation to the forcing to the corresponding values a period later is used.

A grazing impact is an impact with zero velocity. This implies that if a point in the Poincaré section leads to a grazing impact during the following forcing period, some nearby points will either impact with low but non-zero velocity, or will not impact at all. In fact the points leading to grazing impact will in general form a smooth curve L_1 in the Poincaré plane, with impacting points on one side and non-impacting on the other. In the image of this local region under the mapping, the points coming from a grazing impact (the image of L_1) also form a curve L_2 . If a local coordinate system x - y is defined near L_1 , with $x = 0$ representing L_1 , and another local coordinate system X - Y is defined near L_2 , with $X = 0$ representing L_2 , the local form of the mapping will be (Nordmark 1991)

$$\left. \begin{aligned} X &= Ax + \text{higher order terms}, \\ Y &= B\sqrt{-x} + Cy + \text{higher order terms} \end{aligned} \right\} \quad (4)$$

on the impacting side $x < 0$ of L_1 , and

$$\left. \begin{aligned} X &= Dx + \text{higher order terms}, \\ Y &= Ex + Cy + \text{higher order terms} \end{aligned} \right\} \quad (5)$$

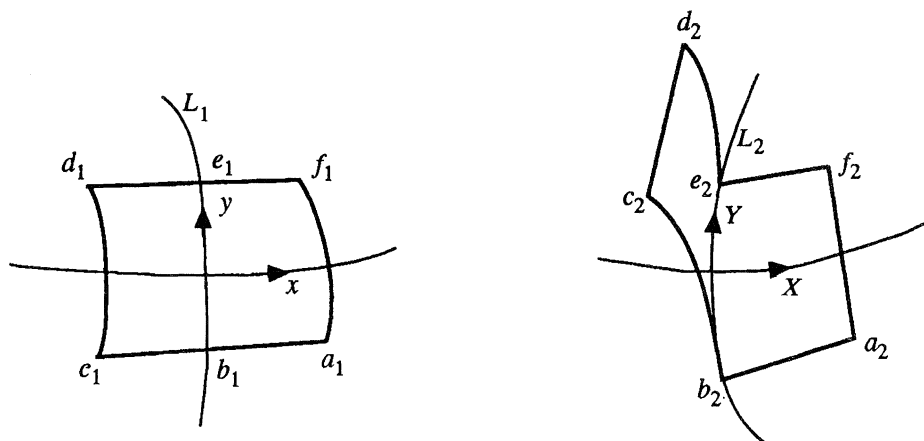


Figure 3. Mapping geometry. The region $a_1 b_1 c_1 d_1 e_1 f_1$ is mapped to the region $a_2 b_2 c_2 d_2 e_2 f_2$.

on the non-impacting side $x > 0$. A , B , C , D are positive constants and E is a constant. The geometric effect of the mapping is shown in figure 3.

The form of the mapping clearly shows that the mapping is singular (although continuous) along L_1 , and the square root term will be a source of large derivatives on the impacting side. As a special example, when the parameter a in the mathematical model is slowly increased through 1, the mass will start to impact. Because of the low velocity of the impacts, the large derivatives will cause the motion to become unstable. The motion will thus change discontinuously and settle down into a motion with some impacts of moderate velocity. A part of this investigation is to verify this behaviour in the experimental system.

4. Experimental setup

The external forcing of the experimental system was sinusoidal, supplied by an electromagnetic shaker from Bruel & Kjaer, type 4809. A large mass was attached to the shaker armature to make the base massive in comparison to the mass so that the impact had minimum effect on the motion of the base. The impact head was made of aluminium in order to avoid the magnetic effects from the shaker.

The mass was a ball-bearing ball made of steel. The spring was made of shim steel with the dimensions $0.5 \text{ mm} \times 12.9 \text{ mm} \times 160 \text{ mm}$. Two shim steel beams with thickness 0.1 mm were stuck on the spring with double-sided adhesive tape to increase the damping.

The excitation and the response were simultaneously measured in V/mm by two inductive displacement transducers from RDP Electronics LTD, type D2/200A and D2/200. The one that gave the motion of the base was guided and the other was unguided in order to disturb the system as little as possible. It was assumed that the system was not influenced by the transducers when the response was small. The signals were processed using a Macintosh IIx. The computer was equipped with an ACM2-12-8A measurement card from Strawberry Tree Computers and the analysis program WorkbenchTM. The displacements were measured as functions of time and they were shown almost instantaneously on the screen. The minimum sampling time was $780 \mu\text{s}$ and the maximum number of measurement points was 178000 in each

measurement. A fast Fourier transform (FFT) analyser was used separately to give the frequency spectrum and autocorrelation of the response.

The velocity of the mass was obtained by differentiating the measured displacement numerically. Because a small error in the displacement gives a larger error in the velocity when the sampling time is small, the signals had to be filtered before the differentiation. The main source of the errors in the measured displacements is the resolution of the AD-converter, since it only allows discrete values of the measured signal. A FIR-(Finite-Duration-Impulse-Response) filter was used. The start transients were also eliminated by matching initial conditions. The filtering decreased the noise and it also smoothed the impact line in the phase plane. The qualitative appearance of the experimentally obtained phase plane histories and Poincaré sections were not influenced by this effect because the characteristics of the motion (periodic or non-periodic motions, maximum amplitudes etc.) were preserved. The filtering would affect quantitative measures such as fractal dimension within chaotic regimes, but these measures were not considered in this investigation. Another possibility to represent the motion is to plot it in the pseudo-phase-space (Moon 1987), i.e. plotting $x(\tau)$ against $x(\tau + T)$, where T is a fixed time constant. In the pseudo-phase-space representation, differentiation of the measured displacement is not needed. However, for a close comparison of the experimentally obtained results and numerical simulations, the Poincaré section representation of the motion in the $x(\tau)$ - $dx(\tau)/d\tau$ plane was found to be the most favourable representation.

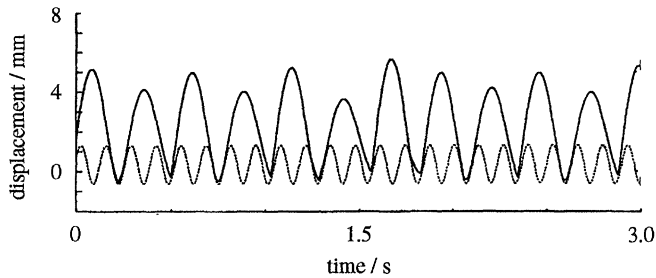
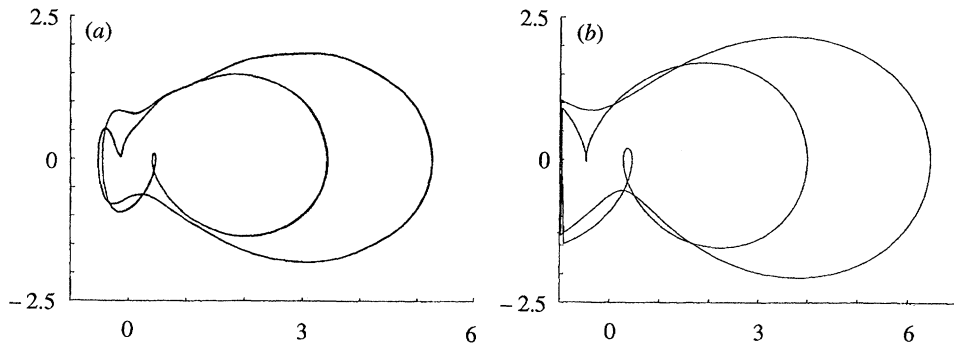
To make it possible to compare experimentally and numerically obtained results, the parameters (coefficient of restitution, lowest natural frequency of the undamped, unforced system and damping) had to be experimentally determined. The equilibrium stand-off distance between the mass and the base was measured before each measurement.

One measurement series was taken for the equilibrium stand-off distance of 1.36 mm. The possible ranges of parameters were small due to equipment limitations on the measurement of the absolute displacement of the mass. To increase the ranges, the equilibrium stand-off distance was decreased to 0.70 mm. The non-dimensionalization makes it possible to put the results in the same diagram since the equilibrium stand-off distance only scales the amplitude of the response. The equipment limitations prevented measurements in the frequency range outside 1.5 and 15.5 Hz, corresponding to w between 0.5 and 5.5. The damping coefficient, D , was found to be 0.057, the natural frequency, ω_n , was 2.79 rad/s and the coefficient of restitution, e , was 0.7.

The experimental equipment was assembled and disassembled and the equilibrium stand-off distance was varied, and the motion (in non-dimensional form) still had the same behaviour. Consequently, the experiment was considered to be repeatable.

5. Numerical simulations

The simulation of the behaviour of equation (1) is based on the known general solution between impacts. The two free constants are chosen to match initial conditions. The time of next impact is found using a modified Newton–Raphson root solving method that guarantees the detection of the first crossing of $x = -1$ (Nordmark 1992*b*). The possible case of the mass coming to rest at $x = -1$ is treated separately.

Figure 4. Experimental time history for $w = 2.71$.Figure 5. Phase plane histories in the $x(\tau)$ - $dx(\tau)/d\tau$ plane for $w \approx 3.0$ (a) experimentally obtained results (b) numerically simulated results.

The local accuracy of the simulation is of machine precision order, and the ability to detect impacts with very low velocity is better than if the equation of motion was integrated numerically.

6. Results

The motion is measured as displacement as a function of time. A typical time history plot is shown in figure 4. The solid line represents the motion of the mass and the dashed line shows the motion of the base. The signals are not filtered.

In the experiments the excitation amplitude was increased until impact started. Thus the non-dimensional amplitude is just above 1. In the numerical simulations the amplitude was chosen to be 1.1.

For comparison with the numerical simulations, the experimental data is non-dimensionalized as in §2. The data is presented in several ways. The motion can be projected onto the x - $dx/d\tau$ plane called a phase plane history. Chaotic motion is most clearly presented as a series of points in a Poincaré section. The Poincaré section used here gives the values of x and $dx/d\tau$ whenever $\tau = \pi/2 \bmod 2\pi$ in the equation of motion. This is whenever the base passes its equilibrium position from positive to negative displacement. To evaluate the motion over a wide range of excitation frequencies, the motion can be presented in bifurcation diagrams.

The effect of filtering the velocity signal is shown in figure 5. The sudden change in velocity at impact was smoothed by the filtering. A small oscillation is observed right after the impact as a small ripple around the large loop. This is caused by the excitation of higher modes of the mass-beam system at the impact. As the oscillation is quickly damped out and does not significantly affect the overall motion, the assumptions in §2 are reasonable.

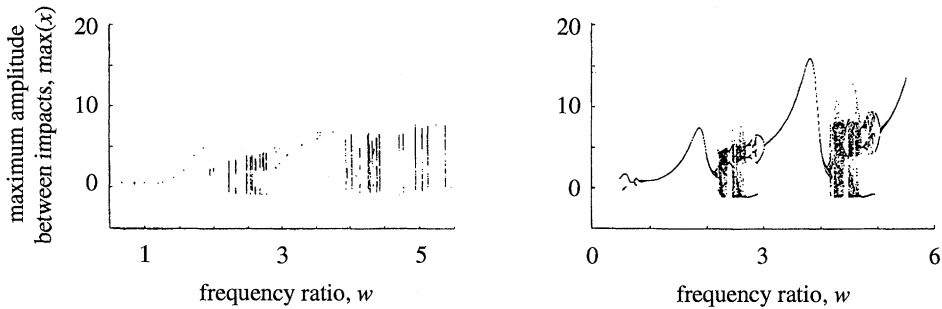


Figure 6. (a) Experimentally obtained and (b) numerically simulated ($a = 1.1$, $D = 0.057$, $e = 0.7$) bifurcation diagrams in non-dimensional form.

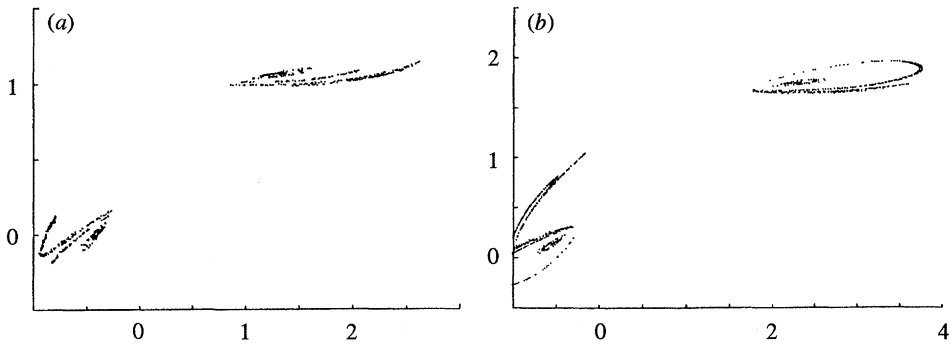


Figure 7. Chaotic attractor for $w \approx 2.6$. Poincaré sections in the $x(\tau)$ – $dx(\tau)/d\tau$ plane for (a) experimentally obtained results (751 points) and (b) numerically simulated results (10000 points).

The difference in scale between the experimentally obtained results and the numerically simulated results is mainly due to the fact that the non-dimensionalized amplitude, $x = (y - z)/b$, is sensitive to measuring errors in the measured displacements $y(t)$, $z(t)$ and the measured initial stand-off distance, b .

In figure 6 a comparison between the experimentally obtained and the numerically determined bifurcation diagram is shown. In the bifurcation diagram the maximum amplitude of the response between each impact is plotted as a function of the frequency ratio, w . Data was recorded after the transients had died out. The bifurcation diagram shows two characteristics of the motion, both the type of response (i.e. number of points) and the maximum amplitudes of the response possible for the specific frequency ratio.

During the experiment the frequency range was swept through (w between 0.5 to 5.5) and the motions were recorded whenever substantial changes in the response were occurring. The numerically determined bifurcation diagram was made using the brute force method for an equally spaced sequence of frequency values. The initial conditions were $x(0) = 1.0$, $dx/d\tau(0) = 1.0$. The diagrams were plotted after the transients had died out.

In figures 7 and 8 two examples of chaotic attractors are shown in the Poincaré section. They are chosen to illustrate how geometric features of the Poincaré mapping that are observed in numerical simulations are also visible in the experimental data. The figures show how the filtering distorts the shape of the attractor near impact. The shape elsewhere and the overall character of the attractor is not affected.

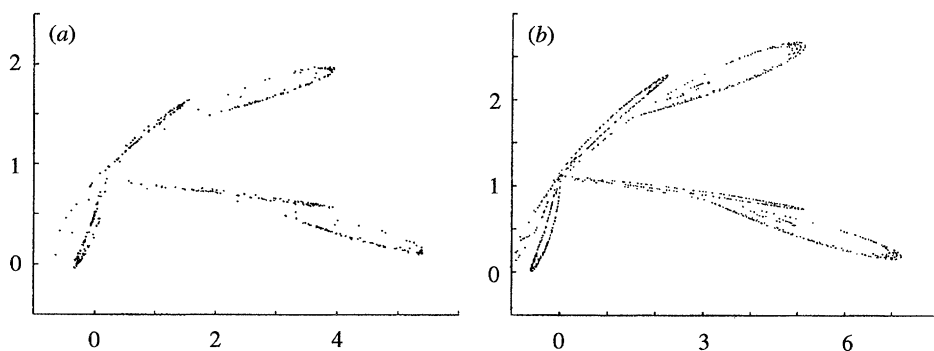


Figure 8. Chaotic attractor for $w \approx 4.3$. Poincaré sections in the $x(\tau)$ - $dx(\tau)/d\tau$ plane for (a) experimentally obtained results (545 points) and (b) numerically simulated results (10000 points).

6. Discussion and conclusions

The behaviour of the system is complex with periodic, subharmonic and chaotic regions, depending on the values of the parameters. When the amplitude was increased until impact started, low amplitude motion of the mass was never observed. This agrees with the expected destabilization caused by the low velocity impact as shown by Nordmark (1991).

It is seen in figures 5–8 that the mathematical model predicts the experimental results well. The good resolution of the measured displacements compared with earlier investigations (for example Shaw 1985*b*) makes it possible to compare the geometric features of the experimentally and theoretically obtained attractors. The discrepancy between the experimentally and the theoretically obtained results near impact, for example, in figure 5, where the velocity suddenly should change, are due to filtering of the measured signal.

The Poincaré section diagrams shown in figures 7 and 8 illustrate geometric features of the attractors unique to models of impacting systems. The curled up structures making up the ‘tips of the fingers’ in figure 8 are signs of the mass undergoing a rapid series of successive impacts, possibly even coming to rest pressed against the base. The finger-like type of attractor has also been found in other impacting models (Thompson & Ghaffari 1983; Shaw 1985*b*). The apparent disconnectedness of the upper right half of the attractor in figure 7, as well as the sharp corner at the same place, are signs of the mass undergoing low velocity, ‘grazing’ impacts (Nordmark 1991, 1992*a, b*). The fact that these features also were found in the experimental results supports that this type of structure in the Poincaré section diagrams is an indication of such impact events playing a strong role in the dynamics. It is to be expected that the identification of such structures in general mechanical systems can be used to diagnose impacts as a feature of the mechanical system under study.

The experimental and theoretical bifurcation diagrams in figures 6*a, b*, respectively, are similar. The larger values in maximum amplitude in figure 6*b* in the frequency ranges 3–4 and 5–6 are due to nonlinear effects in the experiment which are not accounted for in the mathematical model. Large displacements of the mass connected to the spring in figure 1 cause nonlinear characteristics of the spring and additional friction in the inductive displacement transducers.

The series of resonance peaks in figure 6*b* of period n and with a single impact during the period, has been found in similar models (Thompson & Ghaffari 1982;

Shaw & Holmes 1983*b*; Shaw 1985*b*; Moon & Shaw 1983). Approximately, half a period of free oscillations takes place during n periods of forcing, so the peaks occur near $w = 2n$. The motion represented by the resonance peaks can be found analytically (Shaw & Holmes 1983*b*) and the peaks end in period doublings when w is increased or decreased.

To summarize, it is shown in this paper that the single degree of freedom model using an instantaneous impact describes the experimental system well. In particular, the destabilizing effects of the low velocity impacts were observed and the accuracy of the measurements made it possible to identify the geometrical features of the chaotic attractors that are typical for this type of impacting model. Since the experimental system actually has more than one degree of freedom, our measurements support that these features are present in more complex systems. Conversely, the observation of these features in experimental measurements indicate the presence of low velocity impacts in the dynamics of the system.

We thank Professor Lennart Karlsson at the Division of Computer Aided Design at Luleå University of Technology in Sweden and Professor Martin Lesser at the Department of Mechanics at the Royal Institute of Technology in Sweden for supporting this work. We also thank the Volvo Research Foundation for the financial support.

References

- Bayly, P. V. & Virgin, L. N. 1993 An experimental study of an impacting pendulum. *J. Sound Vib.* **164**, 364–374.
- Chen, L. & Semercigil, S. E. 1992 A beam impactor. *J. Sound Vib.* **157** (2), 303–315.
- Holmes, P. J. 1982 The dynamics of repeated impacts with a sinusoidally vibrating table. *J. Sound Vib.* **84** (2), 173–189.
- Isomäki, H. M., Von Boem, J. & Rätty, R. 1985 Devil's attractors and chaos of a driven impact oscillator. *Physics Lett. A* **107** (8), 343–346.
- Kowalik, Z. J., Franaszek, M. & Pieráński, P. 1988 Self-reanimating chaos in the bouncing ball system. *Phys. Rev. A* **37**, 4016–4022.
- Lo, C. C. 1985 A cantilever beam clattering against a stop. *J. Sound Vib.* **69** (2), 245–255.
- Moon, F. C. 1987 *Chaotic vibrations – an introduction for applied scientists and engineers*. New York: John Wiley.
- Moon, F. C. & Shaw, S. W. 1983 Chaotic vibrations of a beam with nonlinear boundary conditions. *Int. J. Nonlinear Mech.* **18**, 465–477.
- Nordmark, A. B. 1991 Non-periodic motion caused by grazing incidence in an impact oscillator. *J. Sound Vib.* **145** (2), 279–298.
- Nordmark, A. B. 1992*a* Effects due to low velocity impact in mechanical oscillators. *Int. J. Bifurcation Chaos* **2** (3), 597–605.
- Nordmark, A. B. 1992*b* Grazing conditions and chaos in impacting systems. Ph.D. thesis ISSN 0348-467X. Royal Institute of Technology, Sweden.
- Peterka, F. 1992 Transition to chaotic motion in mechanical systems with impacts. *J. Sound Vib.* **154** (1), 95–115.
- Shaw, S. W. 1985*a* The dynamics of a harmonically excited system having rigid amplitude constraints (parts 1 & 2). *J. appl. Mech.* **52** (2), 453–464.
- Shaw, S. W. 1985*b* Forced vibrations of a beam with one sided amplitude constraint: theory and experiment. *J. Sound Vib.* **99** (2), 199–212.
- Shaw, S. W. & Holmes, P. J. 1983*a* A periodically forced impact oscillator with large dissipation. *ASME J. appl. Mech.* **5**, 849–857.
- Shaw, S. W. & Holmes, P. J. 1983*b* A periodically forced piecewise linear oscillator. *J. Sound Vib.* **90**, 129–144.

- Shaw, S. W. & Holmes, P. J. 1983*c* Periodically forced linear oscillator with impacts: chaos and long period motions. *Phys. Rev. Lett.* **51**, 623–626.
- Sung, C. K. & Yu, W. S. 1992 Dynamics of a harmonically excited impact damper: bifurcations and chaotic motion. *J. Sound Vib.* **158** (2), 317–326.
- Thompson, J. M. T. 1983 Complex dynamics of compliant off-shore structures. *Proc. R. Soc. Lond. A* **387**, 407–427.
- Thompson, J. M. T. & Ghaffari, R. 1982 Chaos after period-doubling bifurcations in the resonance of an impact oscillator. *Physics Lett. A* **91** (1), 5–8.
- Thompson, J. M. T. & Ghaffari, R. 1983 Chaotic dynamics of an impact oscillator. *Phys. Rev. A* **27**, 1741–1743.
- Whiston, G. S. 1987*a* On the statistics of chaotic vibro-impact. *J. Sound Vib.* **116** (3), 598–603.
- Whiston, G. S. 1987*b* Global dynamics of a vibro-impacting linear oscillator *J. Sound Vib.* **118** (3), 395–424.
- Whiston, G. S. 1992 Singularities in vibro-impact dynamics. *J. Sound Vib.* **152** (3), 427–460.
- Wood, L. A. & Byrne, K. P. 1982 Experimental investigation of a random repeated impact process. *J. Sound Vib.* **85**, 53–69.